Studies of J-PET detector to monitor range uncertainty in proton therapy

A. Ruciński[1], J. Baran[1], J. Gajewski[1], M. Pawlik-Niedźwiecka[1,2], P. Moskal[2]

On behalf of J-PET collaboration

[1]Institute of Nuclear Physics Polish Academy of Sciences, PL-31342 Krakow, Poland

[2]Faculty of Physics, Astronomy and Applied Computer Science, Jagiellonian University, 30-348 Kraków, Poland

INTRODUCTION

Proton beam therapy (PBT) range monitoring is needed to fully exploit the advantages of proton beam in the clinic. In PBT the distribution of β^+ emitters induced by a proton beam in patient can be detected by PET scanners, the emission distribution can be reconstructed and used for monitoring of the beam range.

The aim of this work is to study the feasibility of the new, plastic scintillator based J-PET technology for range verification in PBT. The coincidence events detection efficiency for different setups and examples of reconstructed images will be presented.

MATERIALS AND METHODS

Plastic-scintillator based PET detector

At the Jagiellonian University in Kraków, a novel solution for diagnostic PET imaging, Jagiellonian-PET (J-PET), is being developed. A single detection unit of the J-PET scanner consists of a 50 cm long and 6×24 mm^2 cross section scintillator strips. Light pulses produced by the annihilation photons propagate to strip edges where they are converted into electrical signals by silicon photomultipliers (SiPM). The time of flight (TOF) information between the signals registered at strip ends (by SiPM) is used to estimate the interaction position of the photon with the strip. A J-PET module consists out of 13 strips, signal is read-out through a single front-end electronics and a FPGA-based and DAQ system. Additionally, J-PET technology enables TOF method at the LOR level (Fig.1).

A modular, lightweight and portable design of J-PET modules enables flexibility in detector configuration and easy installation (Fig. 2).

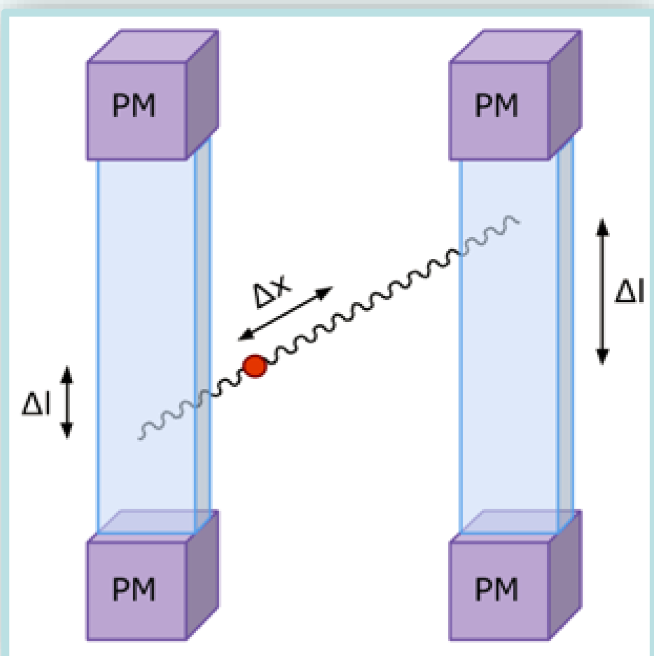

Fig. 1. Scheme of the J-PET concept

Fig. 2. Diagnostic J-PET scanner. Each of 24 modules consists of 13 scintillating strips.

Monte Carlo simulations

GATE Monte Carlo toolkit[1] (ver. 8.2) with Geant4 ver. 10.4.2 have been used to simulate six geometrical configurations of J-PET modules based on modular J-PET system. The efficiency for detection of the β^+ annihilation photons induced in PMMA target (5x5x20cm^3) by a proton beam has beam investigated (Fig. 3). Simulated setups are presented in Fig. 4 and characterized in Table 1.

10^8 primary protons has been simulated for each setup. The QGSP_BIC_HP_EMY physics list was used in simulations. All the coincidences integrated over the time were used for the reconstruction. The energy and time windows were set on 200 keV and 3 ns, respectively.

PET data reconstruction

CASToR software[2] has been used for a 3D reconstruction of β^+ activity distributions. The list-mode TOF-MLEM reconstruction (5 iterations with 500 ps TOF resolution without regularization) was used accounting for random, scatter, attenuation and normalization corrections. The activity map was reconstructed in 2.5 mm^3 isotropic voxel grid.

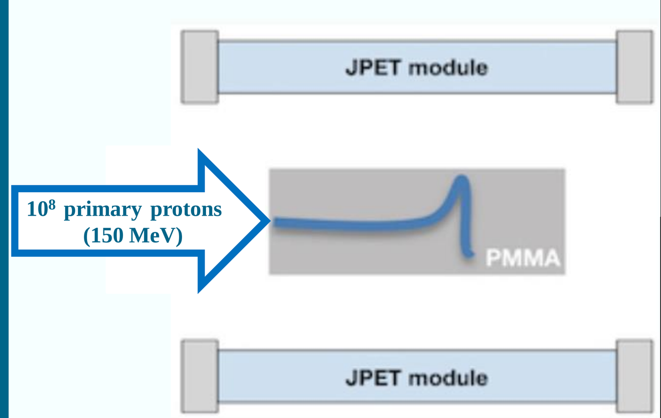

Fig. 3. Schematic view on the simulation setup cross section.

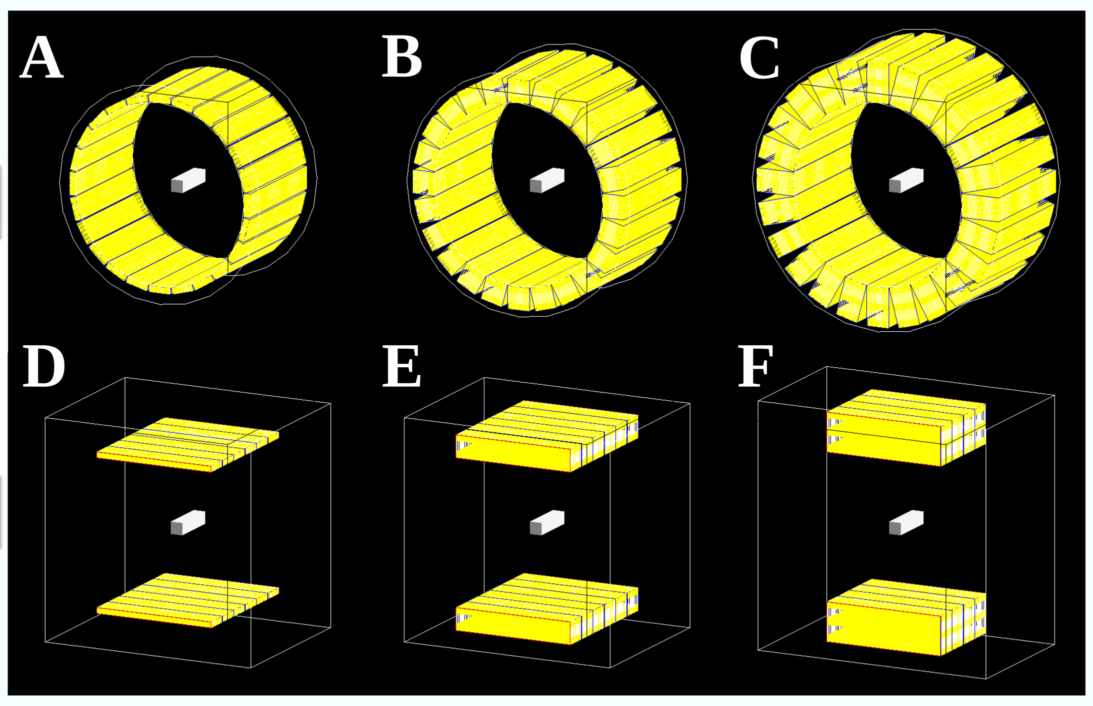

Fig. 4. Simulated J-PET configurations: single layer barrel(A), double layer barrel(B), triple layer barrel (C), single layer dual-head(D), double layer dual-head(E), triple layer dual-head (F)

RESULTS

Coincidence events detection efficiency for different setup

Table 1 lists the total numer of registered coincidence events and integrated over time . True and scattered fractions are distinguished. The comparison between the configurations with the same numer of modules (A,E and F) revealed that greater number of layers have the prevailing effect over the geometrical acceptance.

TABLE 1

CONFIGURATION	NUMBER OF MODULES	GEOMETRICAL ACCEPTANCE	COINCIDENCES		
			ALL	TRUE	SCATTERED
single layer barrel (A)	24	0.39	590	455	94
double layer barrel (B)	48	0.39	1202	943	218
triple layer barrel (C)	72	0.39	1657	1318	285
single layer dual-head (D)	12	0.27	280	231	51
double layer dual-head (E)	24	0.27	948	764	161
triple layer dual-head (F)	24	0.18	1043	871	152

Reconstruction

An example of reconstructed PET images superimposed on CT of homogeneous PMMA phantom for two configurations (double layer barrel and dual-head) are presented in Fig. 5. Reconstructed and true (Monte Carlo) β^+ lateral profiles integrated over the phantom along Z direction for the same two configurations are presented in Fig. 6. The sigmoid function has been fitted to the activity distal fall-offs and the difference between the fall-offs (at the half width maximum) is calculated. Although the small statistics, the calculated differences are below 3 mm and a good agreement between the profiles is observed.

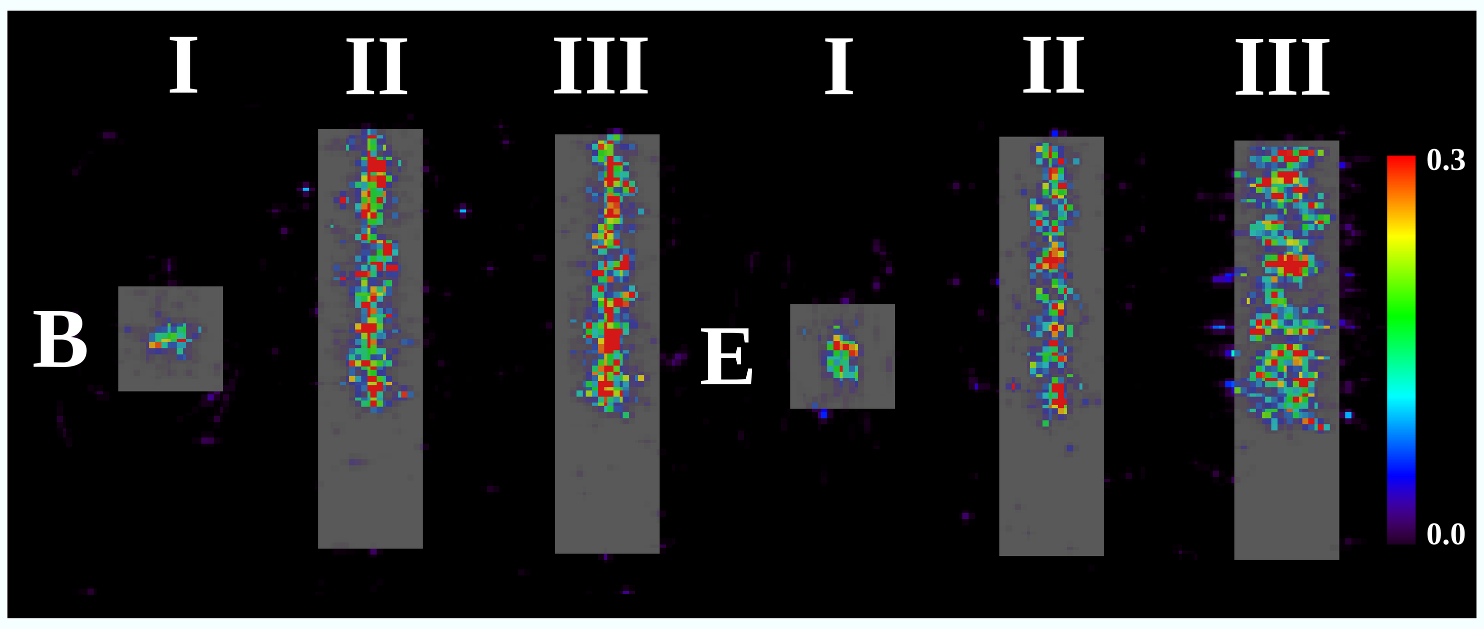

Fig. 5. Normalized reconstructed β^+ profiles for double layer barrel (B) and dual-head (E) configurations in axial (I), coronal (II) and sagittal (III) view

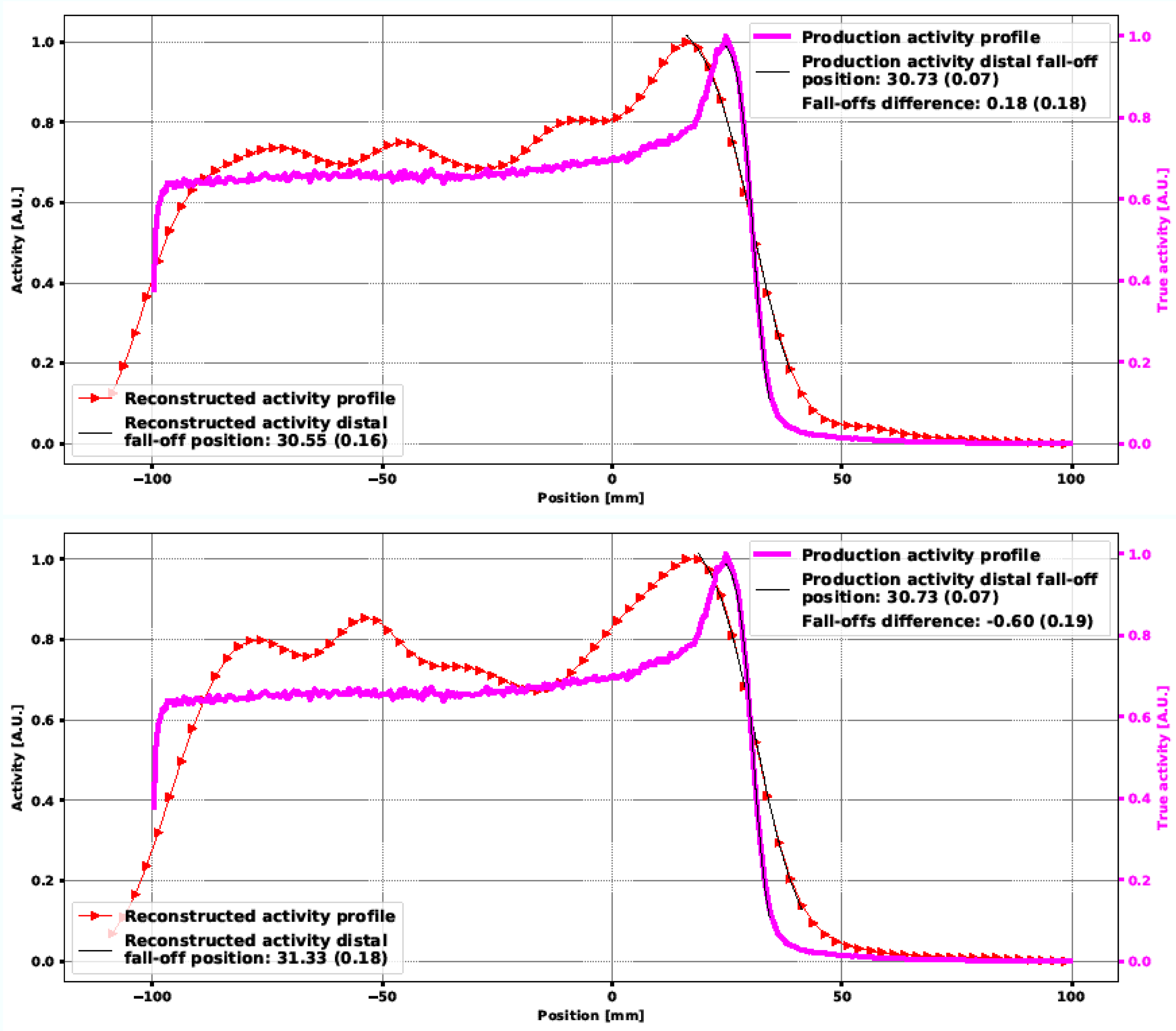

Fig. 6. Normalized reconstructed and true β^+ activity profiles integrated over PMMA phantom along Z direction for: double layer barrel (top) and dual-head (bottom)

CONCLUSIONS

The simulation results show that all presented configurations based on J-PET detector are feasible to acquire the β^+ activity produced by therapeutic proton beams in phantom which are sufficient for 3D reconstruction of PET activity distributions using CASToR. The characterization of J-PET sensitivity for proton beam range detection is currently an ongoing research activity. The future plans include simulations of β^+ activity induced in patient by proton treatment as well as experimental validation of the simulations.

LITERATURE:

[1] Sarrut D., et al. Med. Phys. 2014;41:64301

[2] Merlin T., et al. CASToR: Phys. Med. Biol..2018;63.

[3] Smyrski J., et al. Nucl. Inst. and Meth. in Phys. Res. A. 2017;851:39–42

ACKNOWLEDGEMENTS: Research was supported by: the National Centre for Research and Development (NCBiR), grant no. LIDER/26/0157/L-8/16/NCBR/2017, the Foundation for Polish Science (FNP) co-financed by the EU under the European Regional Development Fund, POIR.04.04.00-00-2475/16-00, TEAM POIR.04.04.00-00-4204/17. J. Baran acknowledges the support of InterDokMed project no. POWR.03.02.00-00-I013/16. This research was supported in part by computing resources of ACC Cyfronet AGH. We acknowledge the support of NVIDIA Corporation with the donation of the GPU used for this research.

IEEE NSS MIC 2019, Manchester, 26 October - 2 November 2019